Finite Element Modeling of Wall Thinning Defects: Applications to Lamb Wave Generation and Interaction

Hyunjo Jeong*[†], Tae-Ho Kim*, Seung-Seok Lee** and Young-Gil Kim**

Abstract The generation of axisymmetric Lamb waves and interaction with wall thinning (corrosion) defects in hollow cylinders are simulated using the finite element method. Guided wave interaction with defects in cylinders is challenged by the multi-mode dispersion and the mode conversion. In this paper, two longitudinal, axisymmetric modes are generated using the concept of a time-delay periodic ring arrays (TDPRA), which makes use of the constructive/destructive interference concept to achieve the unidirectional emission and reception of guided waves. The axisymmetric scattering by the wall thinning extending in full circumference of a cylinder is studied with a two-dimensional FE simulation. The effect of wall thinning depth, axial extension, and the edge shape on the reflections of guided waves is discussed.

Keywords: Wall Thinning, Finite Element Model, Lamb Waves, Hollow Cylinder

1. Introduction

Pipe and tube wall thinning due to FAC (flow accelerated corrosion) has been reported in many nuclear power plants. Monitoring and nondestructive evaluation of wall thinning defects are required for safe operation of nuclear power plants. The ultrasonic guided wave technique has become successful in nondestructive evaluation because of its versatility and global inspection possibility in thin-walled structures. There are several ways to generate guided waves in hollow cylinders. Rose et al. (1994) used variable angle beam transducers for Lamb wave generation and NDE in platelike structures. This is a phase-matched method that is based on the Snell's law. Recently, some linear-array type transducers have been developed for guided wave generation, which is based on the wavelength-matched concept (Kino, 1987). A

comb type transducer (Rose et al., 1998) and an interdigital-type transducer (Monkhouse et al., 1997) have been investigated. This idea has also been used to fabricate a ring-array transducer for axisymmetric guided wave generation in pipes (Rose et al. 1995). However, those array transducers excite and receive the guided waves in their both sides, which may cause difficulties in interpreting which side the reflected signals come from. A more general linear-array-type transducer, the time-delay periodic linear array (TDPLA), has been proposed by Zhu and Rose (Zhu and Rose, 1999), which makes use of the constructive/destructive interference concept to achieve the unidirectional emission and reception of guided waves.

In this paper, the axisymmetric guided waves in isotropic hollow cylinder with the time-delay periodic ring arrays (TDPRA) have been investigated using finite element analyses. Then,

axisymmetric scattering by the wall thinning (corrosion) extending in full circumference of a cylinder is studied with a two-dimensional FE simulation. The effect of wall thinning depth, axial extension, and the edge shape on the reflections of guided waves are discussed.

2. Time-Delay Periodic Ring Arrays and Guided Wave Generation

For axisymmetric loads applied, only the axisymmetric waves with zero circumferential displacements will be excited in the hollow cylinder. Numerical examples of the phase velocity dispersion curve of axisymmetric guided modes have been calculated and are shown in Fig. 1(a). At low frequencies, the L(0,1) and L(0,2) modes are less dispersive, whereas higher order modes are more dispersive and each has its cut-off frequency.

Fig. 1(b) shows the configuration of a general, exterior time-delay periodic ring array (TDPRA). It consists of m spatial periods, each has n rings with the ith ring in each period being connected to the ith signal channel. The mechanism for guided wave generation is as follows: the rings in each period will match the guided wave phases at the discrete points on the surface within the period by successively delaying the excitation signal to each ring (the rule of phase-match); while the repetition of the period in space will tailor the waves into the guided modes with the required wavelength as

well as superpose the waves produced by each period (the rule of wavelength-match).

To achieve the unidirectional emission of guided waves in a simple way, we spatially arrange the rings with equal spacing ($\Delta x = S/n$, where S is the spatial period) along the cylinder axis and temporally arranged the channel signals with equal time delay ($\Delta t = T/n$) between any two succeeded channels. Then, the condition for constructive and destructive interference at the two sides of a TDPRA became quite simple [7] $\Delta x/\lambda = \Delta t/T = 1/n$ where T is the time period of the excitation signal and are same to all channels.

3. FE Prediction for L(0,1) Mode Generation and Propagation

The generation process of axisymmetric guided wave modes in a 3 in., schedule 40 steel pipe (76 mm i.d., 5.5 mm wall thickness) with TDPRAs is simulated using the commercial FE package, ANSYS. The load applied by each ring on the outer surface of the cylinder is a prescribed function of time and is supposed to being uniformly distributed normally in the contact area. The steel pipe is considered isotropic and homogeneous with the longitudinal and shear bulk wave velocities being C_L=5830 m/s and C_S=3170 m/s, respectively (E=202.243 GPa, n=0.29). The density is ν =7800 kg/m^3. The 4-node, isoparametric elements are used.
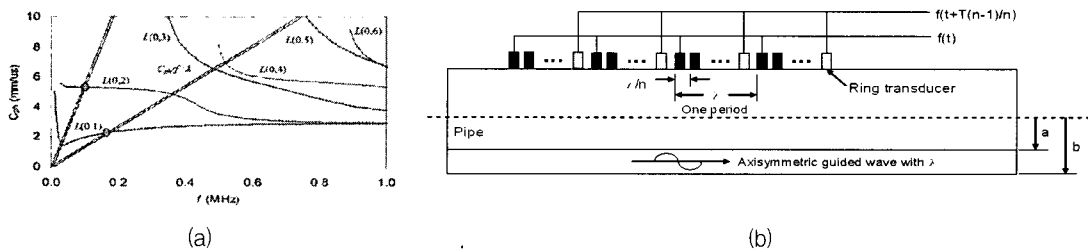

(a)   (b)

Fig. 1 (a) Phase velocity dispersion curves for axisymmetric guided wave modes in a 3 inch, schedule 40 steel pipe (76 mm i.d, 5.5 mm wall thickness), and (b) a time-delay periodic ring array (TDPRA) for axisymmetric guided wave generation in a hollow cylinder

The TDPRA parameters designed for the L(0,1) mode generation are: spatial periods (m)=5, number of rings in each period (n)=4, ring spacing=3.4 mm, ring width=1.7 mm, time delay (T/n)=1.44 s, cycles of toneburst=6, frequency (f)=173.6 kHz, time period (T)= 5.76 ms, phase velocity=2400 m/s, wavelength (λ)=13.6 mm, cylinder length=1190 mm. The toneburst signal is used (Fig. 2) and multiplexed into four channels with 0, T/4, T/2, 3T/4 time delays to drive the TDPRA. The out-of-plane displacements are monitored at a surface point positioned 500 mm away from the TDPRA's center in the enhanced side. The results are shown in Fig. 2. Although the displacement results are not seen in the weakened side, the unidirectional emission has been realized in above 95 percent.

4. Guided Wave Reflections from Axisymmetric Wall Thinnings

To look into the NDT potentials of guided wave modes for wall thinning (corrosion) detection in hollow cylinders, the axisymmetric reflections of the L(0,1) mode is considered. The simulated corrosions are assumed to extend in the full circumference, so that a 2-D axisymmetric FE model can be applied.

Since guided waves can saturate the wall of the hollow cylinder, both outer and inner surface corrosions are included in the simulation. The axisymmetric corrosions are illustrated in Figs. 3 and 4, in which two edge shapes of corrosion zones are considered to test the edge effects: an edge defined by an oblique straight line representing a smooth change of the depth, and an edge defined by a quadratic curve simulating a sharp change in depth. The corrosion depth varies from $\triangle d = 20\%$ to $\triangle d = 80\%$ of the original wall thickness.

First, a smooth corrosion edge on the outer surface is considered which has a depth $\triangle d = 60\%$ of the wall thickness. The center of the TDPRA is placed 508 mm apart from the front edge of the corrosion and the reflected
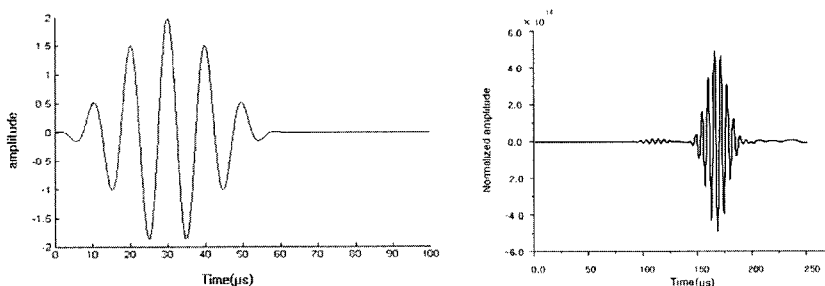

Fig. 2 Input signal of a 6-cycle, 173.6 kHz center frequency toneburst, and predicted L(0,1) mode waveforms received at distance 500 mm away from the TDPRA's center in the enhanced side
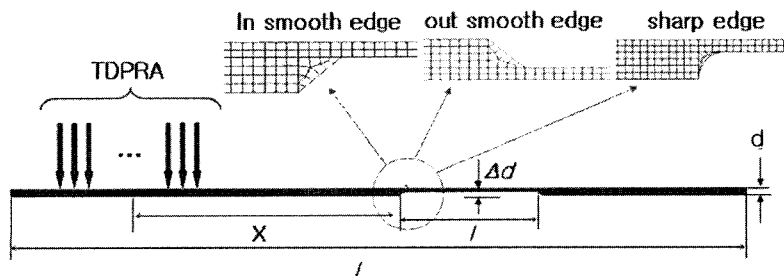

Fig. 3 2-D axisymmetric corrosion defects in a hollow cylinder: (a) inner smooth shape, (b) outer smooth shape, and (c) inner sharp shape. L=2000 mm, x=508 mm, t=5.5 mm, and the corrosion depth $\triangle$d varies from 20% to 80% of the wall thickness t

waves are observed at approximately the middle point between the TDPRA center and the front edge of the corrosion zone. Fig. 5 shows the reflected waves as well as the incident wave, where the out-of-plane displacements are plotted for the $\triangle d = 60\%$ case. It is seen that there are mainly two wavelets in the reflected guided waves, and by examining the times of flight and displacement features, these are identified to be the reflected L(0,1) mode from the front and

rear edges, respectively. It is noted that mode conversion occurs in the corrosion reflection, where the converted L(0,2) is best detected by monitoring its in-plane displacement since its out-of-plane displacement is quite small at the frequency used. Fig. 6 compares the out-of-plane displacements of reflected waves as well as the incident waves for the $\triangle d = 20\%$ and 40%
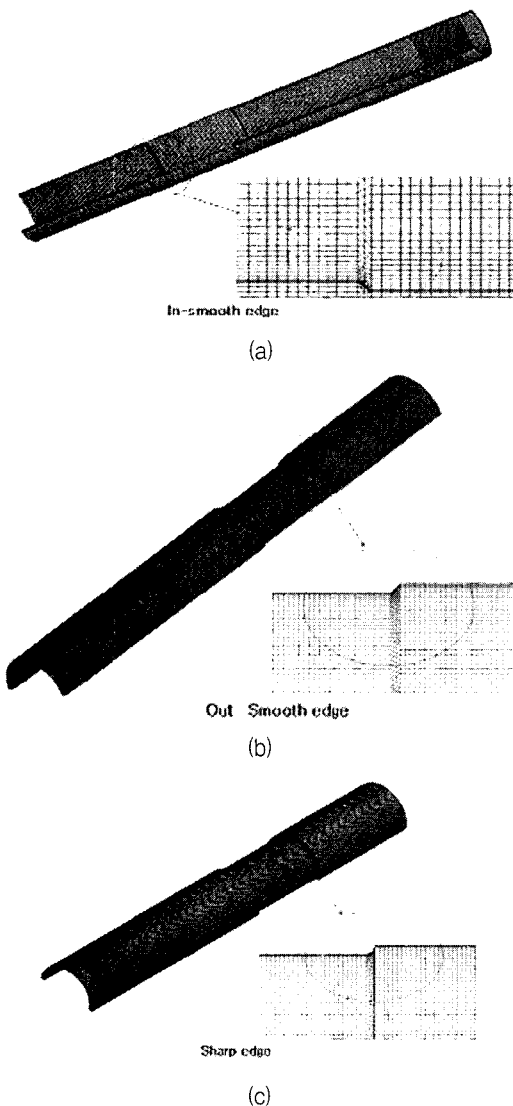

(a)

(b)

(c)

Fig. 4 FE simulation of 2-D axisymmetric corrosion defects in a hollow cylinder: (a) in smooth edge, (b) out smooth edge, and (c) out sharp edge
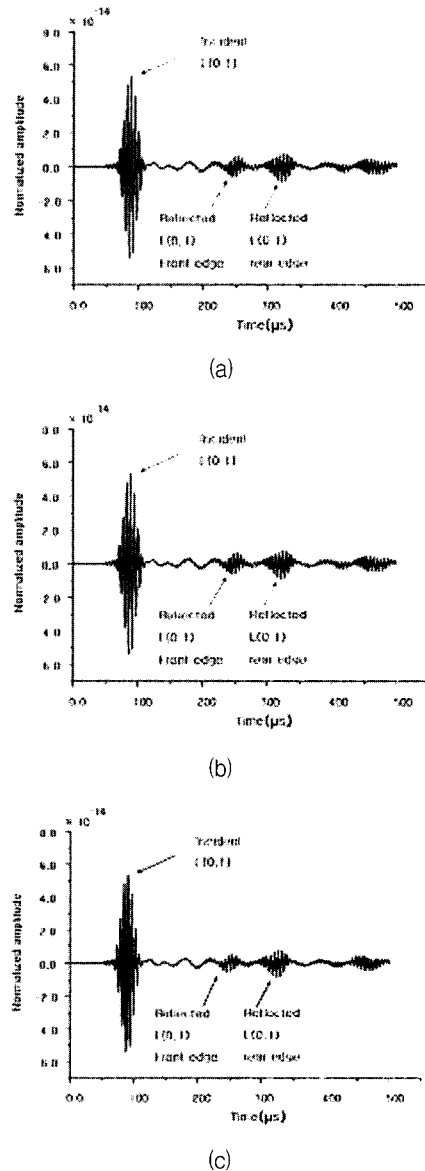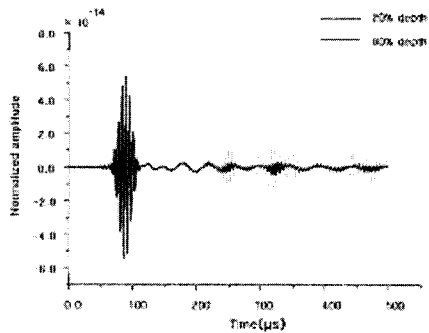

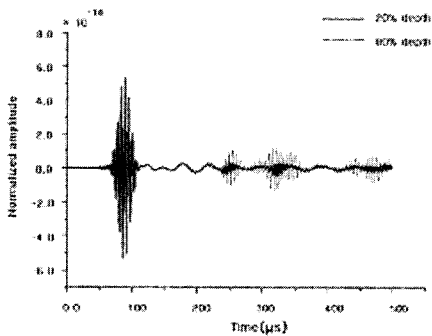(a)

(b)

(c)

Fig. 5 Reflection waves from △d=60% wall thinning under the L(0,1) mode incidence: (a) out smooth edge, (b) in smooth edge, and (c) out sharp edge

cases. It is noticed that the out-of-plane displacements from the front and rear edges of the corrosion increase as the corrosion depth increases.
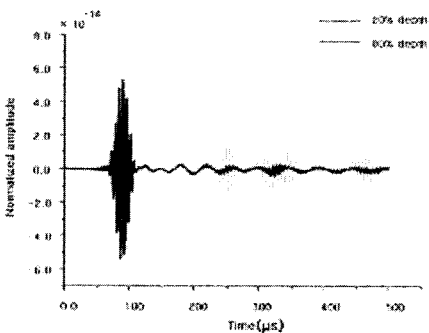
Then, the identical wave incidence is applied to an inner smooth corrosion defect of the same size and shapes, and the reflection waves are monitored also at the same point on the outer surface. The results are also shown in Figs. 5

and 6, which are quite similar to the results of the outer corrosion defect except for the reflected wave amplitude being slightly higher for the inner corrosion. The reflection coefficient of the L(0,1) mode is calculated from the peak amplitude of the reflected wave from the front edge and the incident wave. The results are plotted in Fig. 7 against the corrosion depth for both outer and inner corrosions. Also shown in the figure are the reflection coefficients for an outer corrosion defect with the sharp edges under the same incident wave. The reflection coefficients for the three cases, as shown in Fig. 7, are almost the same until the corrosion depth reaches up to about 60% of the original wall thickness. Above corrosion depths of 60% of the wall thickness, reflections from the two smooth edges continue to remain almost the same, while the sharp edges cause slightly stronger reflections than the smooth edges of the same corrosion depth.

5. Conclusions

The generation of axisymmetric guided waves and their interaction with defects are considered to examine the NDT potentials of these waves for detecting wall thinning due to corrosion in hollow cylinders. The time delayed periodic ring array (TDPRA) model is employed for this
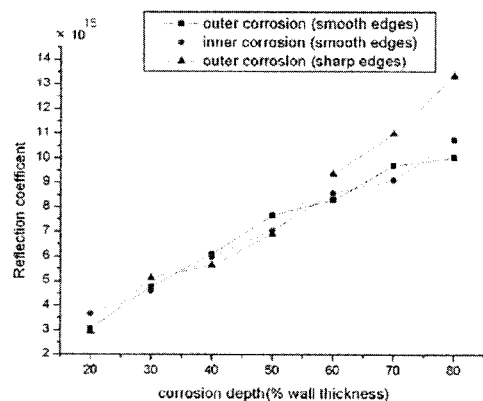

Fig. 6　Reflections from △d=20% and 60% wall thinning under the L(0,1) mode incidence: : (a) out smooth edge, (b) in smooth edge, and (c) out sharp edge

Fig. 7　L(0,1) mode reflection coefficients vs. corrosion depth under the L(0,1) mode incidence

purpose. The finite element simulation of TDPRAs shows that the L(0,1) and L(0,2) modes can be generated efficiently and unidirectionally. Three types of axisymmetric corrosion are simulated for the quantitative study of the relationship between reflected signal amplitudes and wall thinning depths. A fairly linear relationship exists for reflected L(0,1) modes and sharp edges of corrosion zones generally yields stronger reflection signals. Future work should include the study the L(0,2) mode incidence and its reflection. For partial wall thinning (nonaxisymmetric corrosion defects), a 3-D FE simulation is necessary. The TDPRA model is also applicable to the generation of higher order guided waves, and their sensitivity to the wall thinning defects due to corrosion should be studied.

Acknowledgement

References

Kino, G. S. (1987) *Acoustic Waves: Devices, Imaging and Analog Signal Processing,* Prentice-Hall, Englewood Cliffs, NJ, Ch. 4

Monkhouse, R. S. C., Wilcox, P. D. and Cawley, P. (1997) Flexible Interdigital PVDF Transducer for the Generation of Lamb Waves in Structures, *Ultrasonics,* Vol. 35, pp. 489-498

Rose, J. L., Jiao, D. and Spanner, Jr., J. (1996) Ultrasonic Guided Wave NDE for Piping, *Mater. Eval.,* Vol. 54, pp. 1310-1313

Rose, J. L., Pelts, S. P. and Quarry, M. J. (1998) A Comb Transducer Model for Guided Wave NDE, *Ultrasonics,* Vol. 36, pp. 163-168

Rose, J. L., Rajana, K. M. and Carr, F. T. (1994) Ultrasonic Guided Wave Inspection Concepts for Steam Generator Tubing, *Mater. Eval.,* Vol. 52, pp. 307-311

Zhu, W. and Rose, J. L. (1999) Lamb Wave Generation and Reception with Time-Delay Periodic Linear Arrays: A BEM Simulation and Experimental Study, *IEEE Trans. UFFC,* Vol. 46, pp. 654-664

Zhu, W. (2002) An FEM Simulation for Guided Elastic Wave Generation and Reflection in Hollow Cylinders with Corrosion Defects, *J. Pressure Vessel Technology,* Vol. 124, pp. 108-117